NANO LETTERS

Letter

pubs.acs.org/NanoLett

Expeditious Stochastic Calculation of Multiexciton Generation Rates in Semiconductor Nanocrystals

Roi Baer*,† and Eran Rabani*,‡

†Fritz Haber Center for Molecular Dynamics, Chaim Weizmann Institute of Chemistry, The Hebrew University of Jerusalem, Jerusalem 91904 Israel

‡School of Chemistry, The Raymond and Beverly Sackler Faculty of Sciences, Tel Aviv University, Tel Aviv 69978 Israel

ABSTRACT: A stochastic method is developed to calculate the multiexciton generation (MEG) rates in semiconductor nanocrystals (NCs). The numerical effort scales near-linearly with system size allowing the study of MEG rates up to diameters and exciton energies previously unattainable using atomistic calculations. Illustrations are given for CdSe NCs of sizes and energies relevant to current experimental setups, where direct methods require treatment of over 10^{11} states. The approach is not limited to the study of MEG and can be applied to calculate other correlated electronic processes.

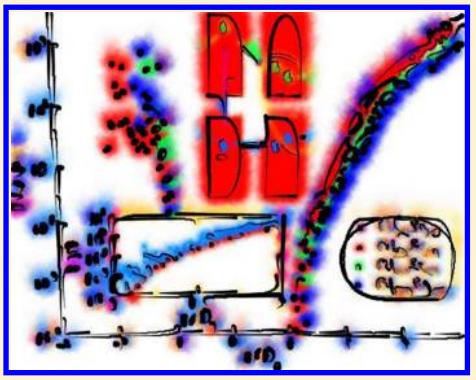

KEYWORDS: *Multiexciton generation, linear scaling, Monte Carlo, spectroscopy of semiconducting nanocrystals*

The electronic, optical, and chemical properties of semiconductor nanocrystals (NCs) are dictated not only by the composite materials but also by their size and geometric shape.[1,2] As a result, prediction and analysis of the interplay of composition, size, shape, and surface effects can be achieved only be detailed atomistic calculations.[3−8] Many of the interesting spectroscopic properties of NCs involve explicit account of electron correlation, requiring consideration of not only the exciton (electron−hole pair) states but also those of multiexcitons (trions, biexcitons, etc.). An example, which introduces further complication, is the estimation of multiexciton generation (MEG) rates following photon absorption in NCs.[9−23] This process involves creation of an electron−hole pair excitation followed by the decay of the electron (or hole) via Coulomb coupling to a trion, composed of two electrons (or holes) and a hole (or electron).[10,12,24] For experimentally relevant NC sizes, the number of pertinent exciton states tops millions per electronvolts and the number of trion states exceeds 10^{10} per electronvolts and the number of Coulomb coupling matrix elements is humongous. Clearly, a method for MEG rate estimation, capable of approaching the exact solution while circumventing the large computational bottleneck, is essential for making progress in this field.

In this paper, we present a new stochastic approach for calculating MEG rates that scales near-linearly with the size of the system. We use the method to study the size dependence of the rates in NCs, reaching diameters and exciton energies previously unattainable by atomistic calculations but significant to a wide range of experiments.[24−40] As an example, we focus on CdSe NCs with diameters up to 5 nm and electron (hole) energies of $4E_g$ above (below) the conduction (valence) band minimum (maximum), where E_g is the fundamental gap.

In our approach, the electronic structure of the NC is based on a single-particle screened pseudopotential model[41] with orbitals $\psi_{r\sigma}(\boldsymbol{r})$ and energies $\varepsilon_{r\sigma}$ (where r = 1, 2,.. and $\sigma = \uparrow,\downarrow$) given by the Schrödinger equation

$$\hat{H}\psi_{r\sigma}(\boldsymbol{r}) = \varepsilon_{r\sigma}\psi_{r\sigma}(\boldsymbol{r}) \tag{1}$$

where $\hat{H} = -[\hbar^2/(2m_e)]\nabla^2 + V(\boldsymbol{r})$ is the single electron Hamiltonian, $V(\boldsymbol{r})$ is the screened pseudopotential, m_e is the electron mass, and $\hbar$ is Planck's constant. Numerically, we use a real-space grid to support the orbitals and screened pseudopotential and fast-Fourier transforms to implement spatial derivatives.[41] For simplicity, we henceforth drop the spin index σ, assuming that the wave functions are spin independent.

In order to treat MEG based on the independent particle model, we use a perturbative approach.[7,14,43] The MEG rate can be estimated from the rate of decay of an exciton S_i^a, describing a hole in state $\psi_i(\boldsymbol{r})$ and an electron in state $\psi_a(\boldsymbol{r})$, into all possible biexcitons B_{jk}^{cb} (describing two holes in states $\psi_j(\boldsymbol{r})$ and $\psi_k(\boldsymbol{r})$ and two electrons in states $\psi_c(\boldsymbol{r})$ and $\psi_b(\boldsymbol{r})$). We use indices i,j,k,l as occupied (hole) state indices, and a,b,c,d as unoccupied (electron) states and r,s,t,u are general indices. Within first order perturbation theory, this is given by rate of

Received: February 3, 2012
Revised: March 19, 2012
Published: March 23, 2012

   dx.doi.org/10.1021/nl300452c | *Nano Lett.* 2012, 12, 2123−2128

formation of all energetically relevant negative and positive trions, $\Gamma_{ia} = \Gamma_i^+ + \Gamma_a^-$ [7,14]

$$\Gamma_a^- = \frac{2\pi}{\hbar}\sum_{cbj} W_{a;cbj}^2 \delta(\varepsilon_a - (\varepsilon_b + \varepsilon_c - \varepsilon_j))$$
$$\Gamma_i^+ = \frac{2\pi}{\hbar}\sum_{jkb} W_{i;jkb}^2 \delta(\varepsilon_i - (\varepsilon_j + \varepsilon_k - \varepsilon_b)) \quad (2)$$

where the coupling elements are

$$W_{i;jkb}^2 = 2|V_{jibk} - V_{kijb}|^2 + |V_{kijb}|^2 + |V_{jibk}|^2$$
$$W_{a;cbj}^2 = 2|V_{acjb} - V_{jcab}|^2 + |V_{jcab}|^2 + |V_{acjb}|^2 \quad (3)$$

These expressions include the effects of spin multiplicity and exchange. In the above equations, the Coulomb matrix elements are

$$V_{rsut} = \int\int d^3r d^3r' \frac{\psi_r(\boldsymbol{r})\psi_s(\boldsymbol{r})\psi_u(\boldsymbol{r}')\psi_t(\boldsymbol{r}')}{\epsilon|\boldsymbol{r} - \boldsymbol{r}'|} \quad (4)$$

and ϵ is the dielectric constant of the NC (in the calculation reported below we use $\epsilon = 5.5$ for all NCs[44]).

Using the above formalism, the trion formation rates Γ_i^+ and Γ_a^- can be calculated directly only if all relevant eigenstates $\psi_{r\sigma}(\boldsymbol{r})$ and eigenenergies ε_r are determined. Presently, this feat can only be done for small NCs, of diameter below 4 nm.[16] The computational bottleneck is caused by the steep increase in the density of states with particle size and photon energy; obtaining all relevant eigenstates and calculating all matrix elements becomes quickly prohibitive due to the huge requirement of computer memory and CPU resources. In addition, one cannot but feel silly in spending such a huge effort, producing each and every one of these eigenstates, whereas not one has a special standing by itself.

An alternative is to use a stochastic approach to sample the initial electron (hole) and final negative (positive) trions involved. The trion formation rate from an electron in state a or a hole in state i can be written as

$$\Gamma_a^- = \frac{2\pi}{\hbar}\langle W_a^2\rangle \rho_T^-(\varepsilon_a)$$
$$\Gamma_i^+ = \frac{2\pi}{\hbar}\langle W_i^2\rangle \rho_T^+(\varepsilon_i) \quad (5)$$

where

$$\rho_T^-(\varepsilon) = \sum_{j,b,c}\delta(\varepsilon - (\varepsilon_b + \varepsilon_c - \varepsilon_j))$$
$$\rho_T^+(\varepsilon) = \sum_{b,j,k}\delta(\varepsilon - (\varepsilon_j + \varepsilon_k - \varepsilon_b)) \quad (6)$$

are the density of negative and positive trions at energy ε, respectively, and $\langle W_a^2\rangle_-$ and $\langle W_i^2\rangle_+$ are the trion-weighted average couplings, formally given by

$$\langle W_a^2\rangle_- = \frac{\sum_{cbj} W_{a;cb,j}^2 \delta(\varepsilon_a - (\varepsilon_b + \varepsilon_c - \varepsilon_j))}{\sum_{cbj}\delta(\varepsilon_a - (\varepsilon_b + \varepsilon_c - \varepsilon_j))}$$
$$\langle W_i^2\rangle_+ = \frac{\sum_{jkb} W_{i;jkb}^2 \delta(\varepsilon_i - (\varepsilon_j + \varepsilon_k - \varepsilon_b))}{\sum_{jkb}\delta(\varepsilon_i - (\varepsilon_j + \varepsilon_k - \varepsilon_b))} \quad (7)$$

Equation 5 shows that trion formation rates depend equally on the trion density of states and the relevant coupling elements. We now discuss how the quantities $\langle W_a^2\rangle_-$, $\langle W_i^2\rangle_-$, $\rho_T^-(\varepsilon)$, and $\rho_T^+(\varepsilon)$ can be computed using stochastic sampling. The densities of trion states (DOTS) can be written as

$$\rho_T^-(\varepsilon) = \int_{\varepsilon_F + E_g}^{\infty} \rho(\varepsilon')\rho_X(\varepsilon - \varepsilon')d\varepsilon'$$
$$\rho_T^+(\varepsilon) = \int_{-\infty}^{\varepsilon_F} \rho(\varepsilon')\rho_X(\varepsilon' - \varepsilon)d\varepsilon' \quad (8)$$

Here, ε_F is the top of the valence band and E_g the fundamental gap of the NC. The density of states at energy ε and the density of excitons at energy $\Delta\varepsilon$ are given by

$$\rho(\varepsilon) = \sum_r \delta(\varepsilon - \varepsilon_r) \quad (9)$$

and

$$\rho_X(\Delta\varepsilon) = \sum_{ia}\delta(\Delta\varepsilon - (\varepsilon_a - \varepsilon_i)) = \int_{\varepsilon_F + E_g}^{\varepsilon_F + \Delta\varepsilon}\rho(E - \Delta\varepsilon)\rho(E)dE \quad (10)$$

respectively. Thus, $\rho_T^-(\varepsilon)$ and $\rho_T^+(\varepsilon)$, the densities of trion states, depend only on the top of the valence band ε_F, the fundamental gap E_g and the density of states $\rho(\varepsilon)$.

In turn, the density of states $\rho(\varepsilon) = tr(\delta(\varepsilon - \hat{H}))$ can be calculated as a limit of the Gaussian function

$$\rho(\varepsilon) = \lim_{\sigma\to 0}\frac{1}{\sqrt{2\pi\sigma^2}} tr\left(e^{-(\hat{H}-\varepsilon)^2/2\sigma^2}\right) \quad (11)$$

In the calculation of the DOS we use a small but finite $\sigma = 0.3$ eV. This causes a small broadening of the DOS, which actually helps to converge the results numerically. Furthermore, various physical effects, such as phonon coupling, have a net broadening effect of this magnitude as well.[7] The DOS can be calculated using a stochastic trace formula as an average over random states ξ[45]

$$tr(f_\varepsilon(\hat{H})) = \langle\langle\xi|f_\varepsilon(\hat{H})|\xi\rangle\rangle_\xi \quad (12)$$

where $f_\varepsilon(\hat{H}) = e^{-((\hat{H}-\varepsilon)^2)/(2\sigma^2)}$, and $\xi(\boldsymbol{r})$ takes a random value of $1/(\Delta V)^{1/2}$ or $-(1/(\Delta V))^{1/2}$ and ΔV is the volume element of the grid. The exponential of the function is performed using Newton interpolation polynomials of order N_c[46]

$$f_\varepsilon(\hat{H}_s)|\xi\rangle \approx \sum_{j=0}^{N_c} a_j(\varepsilon)R_j(\hat{H}_s)|\xi\rangle \quad (13)$$

dx.doi.org/10.1021/nl300452c | Nano Lett. 2012, 12, 2123−2128

where

$$R_j(\hat{H}_s)|\xi\rangle = \prod_{k=0}^{j-1} (\hat{H}_s - h_k)|\xi\rangle \tag{14}$$

and

$$a_0(\varepsilon) = f_\varepsilon(h_0)$$
$$a_1(\varepsilon) = \frac{f_\varepsilon(h_1) - f_\varepsilon(h_0)}{h_1 - h_0}$$
$$a_{j>1}(\varepsilon) = \frac{f_\varepsilon(h_j) - P_{j-1}(h_j)}{R_j(h_j)} \tag{15}$$

In the above equations, h_k are the support points taken to be the zeros of the $N_c + 1$ Chebyshev polynomial.[46] This choice defines the sampling points to lie within the interval $[-2{:}2]$ and $\hat{H}_s$ is a shifted and rescaled $\hat{H}$ having its spectrum of eigenvalues lying in this interval as well.[46] The length of our Newton polynomial is $N_c = 7.7\Delta E/\sigma$ where ΔE is the energy range of the Hamiltonian.[47] For $\rho(\varepsilon)$ we used $N_c = 8192$. Obviously, most of the computational effort goes into the repeated evaluation of $R_j(\hat{H})|\xi\rangle$. Critically, since in eq 13 only the coefficients a_j depend on ε, it is possible to use the same $R_j(\hat{H})|\xi\rangle$ with different expansion coefficients $a_j(\varepsilon)$ to evaluate the $f_\varepsilon(\hat{H})$ at many desired values of ε. This speeds up the calculation by an order of magnitude or two (limited only by the computer memory). In the calculation we obtain the DOS at all desired energies from a single interpolation starting from ξ, and averaging over 500 initial ξs. The statistical error drops quite rapidly and already after 10 ξs a reasonable, estimate of the DOS emerges.

The upper panel of Figure 1 shows the DOS $\rho(\varepsilon)$ as function of energy for several CdSe NCs of varying sizes calculated by the stochastic trace formula (eq 12). The hole states below the Fermi level are lumped into two narrow bands, consistent with the larger effective mass holes have in bulk CdSe. The density of electron states is structured near the band edge rapidly growing into a dense broad continuum, ever denser as energy grows. This DOS grows as D^2 at a scaled energy ε/E_g and as D^3 at absolute energy ε, where D is the diameter of the NC.

The density of excitons $\rho_X(\Delta\varepsilon)$ calculated from eq 10 is shown for these systems in the lower panel of Figure 1. This calculation requires knowledge, not only of $\rho(\varepsilon)$ but also of ε_F and E_g. These latter quantities were obtained by applying similar Gaussian function filters with target energies ε positioned near the top (bottom) of the bulk valence (conduction) band. The length of the polynomial for this calculation was $N_c = 16384$. The results for E_g and ε_F are summarized in Table 1. $\rho_X(\Delta\varepsilon)$ rises rapidly for exciton energies above E_g and plateaus beyond $\sim 4E_g$. This is caused by the gap in the DOS of the holes. For smaller NCs and low exciton energies we also calculated ρ_X using the eigenvalues of the Hamiltonian obtained by the filter-diagonalization method,[47,48] and the two methods yield very similar results. For energies above $\sim 3E_g$ the filter-diagonalization underestimates the density of excitons because at these energies the method fails to locate all eigenenergies due to the high DOS.

In Figure 2 we plot the DOTS $\rho_T^{\pm}$ calculated from the convolutions given by eqs 8 and 10. Positive and negative energies show $\rho_T^-(\varepsilon_F + E_g + \varepsilon)$ and $\rho_T^+(\varepsilon_F - \varepsilon)$, respectively. Both are plotted from the edge of the corresponding bands. For the two smallest NCs the results are compared to those based on eigenenergies, showing good agreement, except at very low energies where the discrete nature of the DOTS is smeared by the finite σ broadening (eq 11). The DOTS grows approximately as D^6 at a scaled energy ε/E_g, resulting from the quadratic scaling of the DOS with D discussed above. Furthermore, the DOTS first grows and then levels out as the energy deviates from the band edge, the latter effect is due to the high-energy plateau of ρ_X (see Figure 1). We also find that $\rho_T^-(\varepsilon_F + E_g + \varepsilon) < \rho_T^+(\varepsilon_F - \varepsilon)$ consistent with previous calculations for smaller NCs.[16]

Calculation of the positive and negative trion formation rates requires, in addition to the DOTS, the calculation of $\langle W_i^2\rangle_+$ and $\langle W_a^2\rangle_-$ given by eq 7. The structure of these equations suggests the use of a stochastic sampling procedure. For the negative trions at energy $\varepsilon_a > \varepsilon_F + 2E_g$ the following procedure was used

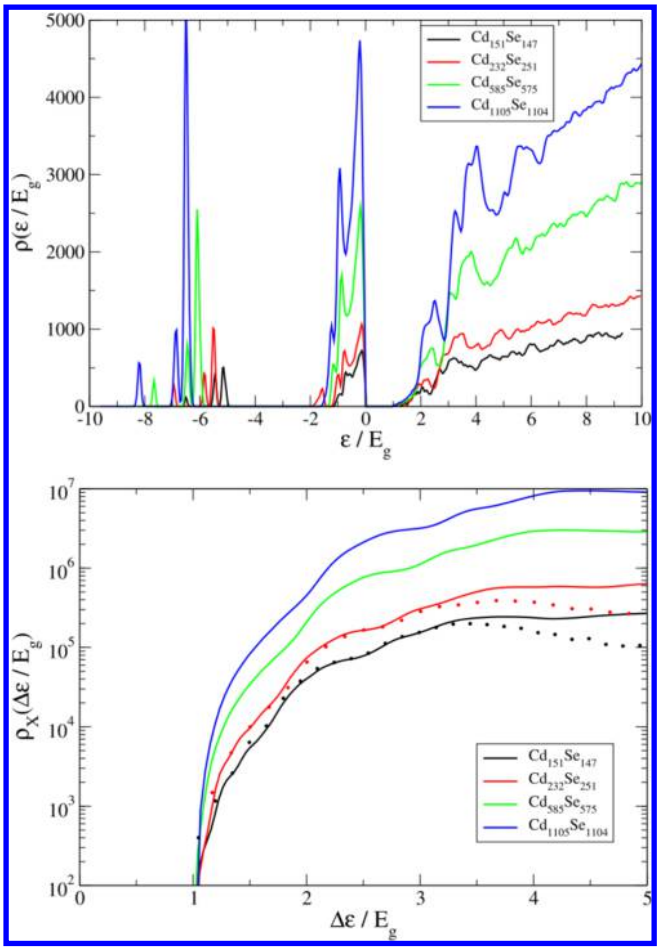

Figure 1. (Top) The DOS $\rho(\varepsilon)$ as a function of scaled energy $\Delta\varepsilon/E_g$ for four CdSe NCs of varying sizes. Zero is taken at the Fermi energy of each NC. (Bottom) The density of excitons $\rho_X(\Delta\varepsilon)$. The lines depict the result from the convolution of the DOS given by eq 10 and the dots are results obtained from the eigenenergies.

Table 1. The Diameter D, Fermi Energy ε_F, and Fundamental Gap E_g for the NCs in This Study

	D (nm)	ε_F (eV)	E_g (eV)
$Cd_{151}Se_{147}$	2.6	−6.4	2.7
$Cd_{232}Se_{251}$	3.0	−6.3	2.6
$Cd_{585}Se_{575}$	4.1	−6.3	2.3
$Cd_{1105}Se_{1104}$	5.0	−6.3	2.2

dx.doi.org/10.1021/nl300452c | Nano Lett. 2012, 12, 2123−2128

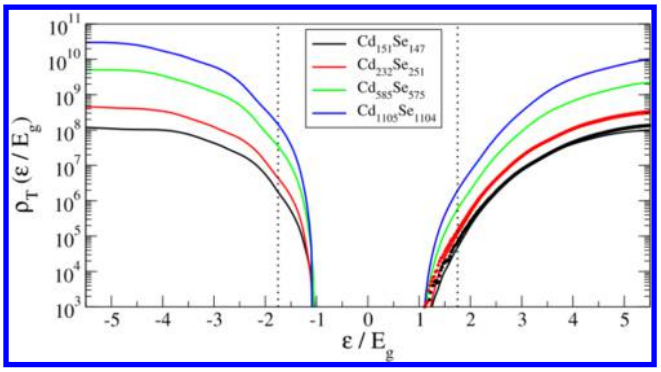

Figure 2. The DOTS in units of the gap E_g for the different NCs based on eqs 8 and 10. Positive and negative energies correspond to density of negative trions $\rho_T^-(\varepsilon_F + E_g + \varepsilon)$ measured from the bottom of the conduction band and positive trions $\rho_T^+(\varepsilon_F - \varepsilon)$ measured from the top of the valence band, respectively. Symbols (black and red) are results obtained from nonstochastic (eigenenergy) calculations. The horizontal lines depict the energy range of the calculations in refs 7 and 16.

to randomly select a trion that satisfies the resonance condition $\varepsilon_b + \varepsilon_c - \varepsilon_j = \varepsilon_a$:

(1) Select a random energy $\varepsilon_c \in [\varepsilon_F + E_g, \varepsilon_a - E_g]$
(2) Select a random energy $\varepsilon_j \in [\varepsilon_F - (\varepsilon_a - \varepsilon_c - E_g), \varepsilon_F] = [\varepsilon_F + E_g + \varepsilon_c - \varepsilon_a, \varepsilon_F]$
(3) Set: $\varepsilon_b = \varepsilon_a - (\varepsilon_c - \varepsilon_j)$

For each of the energies ε_b, ε_c, ε_j, and ε_a we apply a Gaussian filter to a random ψ, thus obtaining four near-eigenstates from which $W^2_{a;cbj}$ can be calculated (eq 3). Repeating this procedure and averaging over the $W^2_{a;cbj}$ gives the estimate of $\langle W^2_a \rangle_-$ in eq 7.

A similar procedure applies for the positive trions with the following selection procedure $\varepsilon_i < \varepsilon_F - E_g$ such that $\varepsilon_j + \varepsilon_k - \varepsilon_b = \varepsilon_i$

(1) Select a random energy $\varepsilon_k \in [\varepsilon_i + E_g, \varepsilon_F]$
(2) Select a random energy $\varepsilon_b \in [\varepsilon_F + E_g, \varepsilon_F + \varepsilon_k - \varepsilon_i]$
(3) Set: $\varepsilon_j = \varepsilon_i + (\varepsilon_k - \varepsilon_b)$

Again, for each of the energies ε_j, ε_k, ε_b, and ε_i apply a Gaussian filter to a random ψ, thus obtaining four near-eigenstates from which $W^2_{i;jkb}$ can be calculated (eq 3). Repeating this procedure and averaging over the $W^2_{i;jkb}$ gives the estimate of $\langle W^2_i \rangle_+$ in eq 7.

The Gaussian filter is applied using the Newton interpolation procedure described above with $N_c = 8192$. To further reduce the computational effort, many states can be computed simultaneously with the same interpolation polynomial with different expansion coefficients as discussed above. Thus, we selected 10 negative and 10 positive trions before applying a single Newton expansion. We repeat this procedure 500 times to converge the average values of $\langle W^2_{a,i} \rangle_{-,+}$ to within a small statistical error. However, qualitative results are obtained already after approximately 20 MC iterations.

In Figure 3, we plot the rates of positive and negative trion formation for several CdSe nanocrystals up to diameter of 5 nm and up to energies of $4E_g$ above the conduction band minimum and $3E_g$ below the valence band maximum. For the largest system, a similar calculation using a direct approach with all eigenstates requires approximately 10^5 states represented on grid of $128 \times 128 \times 128$. This is currently beyond conventional computational resources (even on a supercomputer), while the

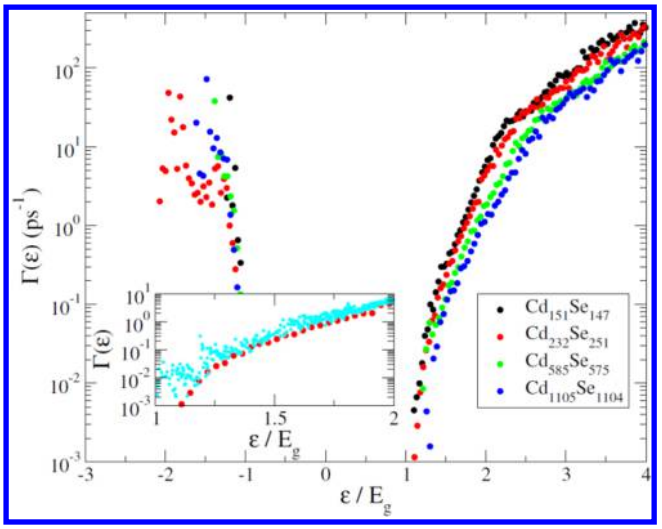

Figure 3. Positive and negative trion formation rates from the stochastic sampling method for several CdSe NCs up to 5 nm in diameter. The positive rates are shown at negative energies measured from the top of the valence band. The negative rates are shown at positive energies measured from the bottom of the conduction band. Inset: Comparison of the negative trion formation rates for $Cd_{232}Se_{251}$ obtained from the TRMC and the direct approach of ref 2.

present stochastic sampling method accomplishes this task utilizing a single core i7 processor with 4GB memory only.

The results for the negative trion formation rates indicate that smaller NCs have larger rates at a given scaled energy, consistent with our previous studies at a lower energy range. The positive trion rates also show a similar trend, though the results are much noisier.[49] An exception to this rule is the positive trion rates for $Cd_{232}Se_{251}$, which fall below the results for the other NCs due to differences in the valence band DOS resulting from the larger asymmetry in the NC composition.

For the energy range shown we find that the trion formation rates scale as D^{-2} for a given scaled energy, indicating that even the largest NC is far from the bulk limit. At a given absolute energy the rates scale as D, signifying the difference in behavior when the energy axis is scaled by the band gap energy, as discuss in the literature. The inset of Figure 3 shows a comparison of the stochastic sampling method with a calculation using all eigenstates for the NC of diameter ~3 nm at energies below $2E_g$. The agreement between the stochastic method and the exact result is very good, albeit the former estimates appear to be a low bound. This behavior is currently not completely understood.

In Figure 4, we plot $(\langle W^2_a \rangle_-)^{1/2}$ for the different NCs calculated using the stochastic sampling procedure. We find that $(\langle W^2_a \rangle_-)^{1/2}$ displays an overall decay for all NCs as the energy increases. Furthermore, the magnitude of the coupling decreases with the NC diameter, approximately as D^{-4}. This is different in comparison with our previous study, where the scaling of $(\langle W^2_a \rangle_-)^{1/2}$ was estimated to close to D^{-3}. The differences are traced to the smaller NCs studied at a limited energy range near E_g. The overall scaling behavior of the different factors entering Fermi's golden rule are summarized in Table 2.

In summary, we have presented a computational method for studying MEG rates in large nanocrystals based on stochastic sampling techniques scaling near-linearly with system size. Using it we were able to determine size and energy dependence

dx.doi.org/10.1021/nl300452c | Nano Lett. 2012, 12, 2123−2128

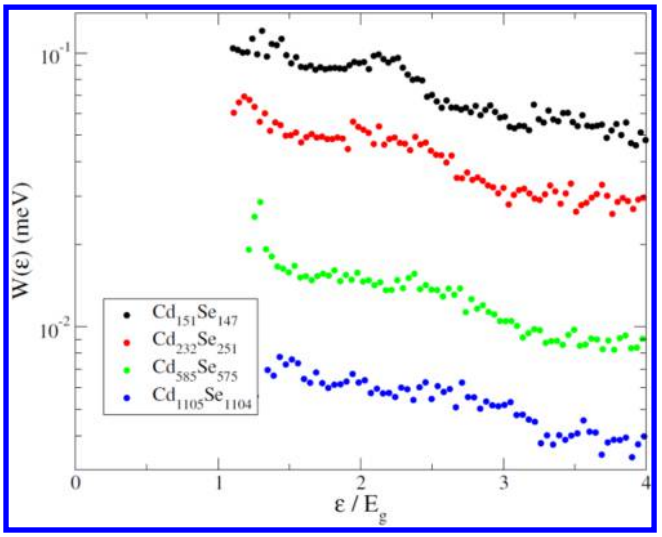

Figure 4. Energy dependence of the square root of $\langle W_a^2 \rangle_-$ for several NCs (cf., eq 7). Energy measured from the bottom of the conduction band.

Table 2. Scaling of $\langle W_a^2 \rangle_-$, ρ_T^-, and Γ_a^- at Energies between E_g and $4E_g$

	$\langle W_a^2 \rangle_-$	ρ_T^-	Γ_a^-
scaled energy (ε/E_g)	D^{-8}	D^{-6}	D^{-2}
absolute energy (ε)	D^{-8}	D^{-9}	D

of MEG rates for CdSe NCs inaccessible before. The method is not limited to these sizes/energies and can be used for even larger systems and various nanoparticle shapes and materials compositions. More importantly, the principles of our approach can be used for developing new electron-correlation methods applicable for other types of rate processes in large systems.

AUTHOR INFORMATION

Notes

The authors declare no competing financial interest.

ACKNOWLEDGMENTS

This research was supported by the Israel Science Foundation (Grants 611/11, 1020/10). E.R. would like to thank the Center for Re-Defining Photovoltaic Efficiency Through Molecule Scale Control, an Energy Frontier Research Center funded by the U.S. Department of Energy, Office of Science, Office of Basic Energy Sciences under Award Number DE-SC0001085.

REFERENCES

(1) Alivisatos, A. P. *Science* **1996**, *271*, 933.
(2) Alivisatos, A. P. *J. Phys. Chem.* **1996**, *100*, 13226.
(3) Zunger, A. *Phys. Status Solidi B* **2001**, *224*, 727.
(4) Prezhdo, O. V. *Acc. Chem. Res.* **2009**, *42*, 2005.
(5) Chelikowsky, J. R. *J. Phys. D: Appl. Phys.* **2000**, *33*, R33.
(6) Rubio, A.; Alonso, J. A.; Blase, X.; Louie, S. G. *Int. J. Mod. Phys. B* **1997**, *11*, 2727.
(7) Rabani, E.; Baer, R. *Chem. Phys. Lett.* **2010**, *496*, 227.
(8) Baer, R.; Rabani, E. *Nano Lett.* **2010**, *10*, 3277.
(9) Isborn, C. M.; Kilina, S. V.; Li, X. S.; Prezhdo, O. V. *J. Phys. Chem. C* **2008**, *112*, 18291.
(10) Franceschetti, A.; An, J. M.; Zunger, A. *Nano Lett.* **2006**, *6*, 2191.
(11) Shabaev, A.; Efros, A. L.; Nozik, A. J. *Nano Lett.* **2006**, *6*, 2856.
(12) Allan, G.; Delerue, C. *Phys. Rev. B* **2006**, *73*, 205423.
(13) Califano, M.; Franceschetti, A.; Zunger, A. *Phys. Rev. B* **2007**, *75*, 115401.
(14) Rabani, E.; Baer, R. *Nano Lett.* **2008**, *8*, 4488.
(15) Pijpers, J. J. H.; Ulbricht, R.; Tielrooij, K. J.; Osherov, A.; Golan, Y.; Delerue, C.; Allan, G.; Bonn, M. *Nat. Phys.* **2009**, *5*, 811.
(16) Lin, Z. B.; Franceschetti, A.; Lusk, M. T. *ACS Nano* **2011**, *5*, 2503.
(17) Korkusinski, M.; Voznyy, O.; Hawrylak, P. *Phys. Rev. B* **2011**, *84*, 155327.
(18) Fischer, S. A.; Prezhdo, O. V. *J. Phys. Chem. C* **2011**, *115*, 10006.
(19) Allan, G.; Delerue, C. *ACS Nano* **2011**, *5*, 7318.
(20) Witzel, W. M.; Shabaev, A.; Hellberg, C. S.; Jacobs, V. L.; Efros, A. L. *Phys. Rev. Lett.* **2010**, *105*, 137401.
(21) Piryatinski, A.; Velizhanin, K. A. *J. Chem. Phys.* **2010**, *133*, 084508.
(22) Korkusinski, M.; Voznyy, O.; Hawrylak, P. *Phys. Rev. B* **2010**, *82*, 245304.
(23) Fischer, S. A.; Madrid, A. B.; Isborn, C. M.; Prezhdo, O. V. *J. Phys. Chem. Lett.* **2010**, *1*, 232.
(24) Ellingson, R. J.; Beard, M. C.; Johnson, J. C.; Yu, P. R.; Micic, O. I.; Nozik, A. J.; Shabaev, A.; Efros, A. L. *Nano Lett.* **2005**, *5*, 865.
(25) Beard, M. C.; Knutsen, K. P.; Yu, P. R.; Luther, J. M.; Song, Q.; Metzger, W. K.; Ellingson, R. J.; Nozik, A. J. *Nano Lett.* **2007**, *7*, 2506.
(26) Schaller, R. D.; Klimov, V. I. *Phys. Rev. Lett.* **2004**, *92*, 186601.
(27) Schaller, R. D.; Petruska, M. A.; Klimov, V. I. *Appl. Phys. Lett.* **2005**, *87*, 253102.
(28) Schaller, R. D.; Agranovich, V. M.; Klimov, V. I. *Nat. Phys.* **2005**, *1*, 189.
(29) Klimov, V. I. *J. Phys. Chem. B* **2006**, *110*, 16827.
(30) Schaller, R. D.; Sykora, M.; Pietryga, J. M.; Klimov, V. I. *Nano Lett.* **2006**, *6*, 424.
(31) Murphy, J. E.; Beard, M. C.; Norman, A. G.; Ahrenkiel, S. P.; Johnson, J. C.; Yu, P. R.; Micic, O. I.; Ellingson, R. J.; Nozik, A. J. *J. Am. Chem. Soc.* **2006**, *128*, 3241.
(32) Pijpers, J. J. H.; et al. *J. Phys. Chem. C* **2007**, *111*, 4146.
(33) Schaller, R. D.; Pietryga, J. M.; Klimov, V. I. *Nano Lett.* **2007**, *7*, 3469.
(34) Ben-Lulu, M.; Mocatta, D.; Bonn, M.; Banin, U.; Ruhman, S. *Nano Lett.* **2008**, *8*, 1207.
(35) Nair, G.; Geyer, S. M.; Chang, L. Y.; Bawendi, M. G. *Phys. Rev. B* **2008**, *78*, 125325.
(36) Nair, G.; Bawendi, M. G. *Phys. Rev. B* **2007**, *76*, 081304.
(37) Nair, G.; Chang, L. Y.; Geyer, S. M.; Bawendi, M. G. *Nano Lett.* **2011**, *11*, 2145.
(38) Sambur, J. B.; Novet, T.; Parkinson, B. A. *Science* **2010**, *330*, 63.
(39) Delerue, C.; Allan, G.; Pijpers, J. J. H.; Bonn, M. *Phys. Rev. B* **2010**, *81*, 125306.
(40) Semonin, O. E.; Luther, J. M.; Choi, S.; Chen, H. Y.; Gao, J. B.; Nozik, A. J.; Beard, M. C. *Science* **2011**, *334*, 1530.
(41) Rabani, E.; Hetenyi, B.; Berne, B. J.; Brus, L. E. *J. Chem. Phys.* **1999**, *110*, 5355.
(42) Jaeger, H. M.; Fischer, S.; Prezhdo, O. V. *J. Chem. Phys.* **2012**, *136*, 064701.
(43) The present approach is based on a single reference ground state and treats electron correlation in a perturbative manner. Other approaches are possible, based on highly corrleated ground state wave fiunctions (see refs 9, 23, and 42 for applications to Si, CdSe, and PbSe clusters).
(44) Wang, L. W.; Zunger, A. *Phys. Rev. B* **1996**, *53*, 9579.
(45) Baer, R.; Seideman, T.; Ilani, S.; Neuhauser, D. *J. Chem. Phys.* **2004**, *120*, 3387.
(46) Kosloff, R. *Annu. Rev. Phys. Chem.* **1994**, *45*, 145.
(47) Wall, M. R.; Neuhauser, D. *J. Chem. Phys.* **1995**, *102*, 8011.
(48) Toledo, S.; Rabani, E. *J. Comp. Phys* **2002**, *180*, 256.
(49) This is because we sample the initial state and the trion state from a uniform distribution within a predefined energy window. Since the width of the valance band is narrow (diminishes below $\varepsilon_F - 2E_g$), there are only very few states that fall within the sampling window. In

future applications, this can be improved by sampling trion states that are weighted by the DOS.

dx.doi.org/10.1021/nl300452c | *Nano Lett.* 2012, 12, 2123−2128